NUMERICAL MODELLING OF TIME-HARMONIC SEISMIC WAVE FIELDS IN SIMPLE STRUCTURES BY THE GAUSSIAN BEAM METHOD. PART I.

JANA KONOPÁSKOVÁ

Geophysical Institute, Czechosl. Acad. Sci., Prague)*

VLASTISLAV ČERVENÝ

*Institute of Geophysics, Charles University, Prague**)*

Резюме: *Метод гауссовских пучков используется для численного моделирования сейсмических волновых полей в некоторых простых моделях среды. Главное внимание уделяется волнам отраженным от плоской границы раздела, особенно области начальной точки. Сравнение с точными решениями показывает, что метод гауссовских пучков дает достаточно точные результаты даже в сингулярной области начальной точки (см. рис. 9б). В закритической области, суммированием гауссовских пучков отраженных волн получаются даже головные волны. В другой части этой работы будет обсуждаться чувствительность результатов к разным параметрам расчетов, напр. к начальной ширине гауссовских пучков, к параметрам суммирования гауссовских пучков, итд.*

1. INTRODUCTION

In the Gaussian beam method, the complete time-harmonic high-frequency seismic wave field in laterally inhomogeneous media generated by a point (or line) source is evaluated as a superposition of Gaussian beams. The Gaussian beams used in these computations are asymptotic high-frequency one-way solutions of elastodynamic equations concentrated close to rays of P and S waves. The elastodynamic equation in this case is reduced to a parabolic equation, so that the Gaussian beams are obtained as solutions of the parabolic equation. The amplitude profile of the principal displacement component of the Gaussian beam perpendicular to the ray is bell-shaped (Gaussian), with the maximum amplitude at the central ray of the Gaussian beam. This is the reason why these solutions are called Gaussian beams. Gaussian beams are regular along the whole ray, including the caustic. More details on elastodynamic Gaussian beams can be found in [1—4].

The evaluation of the wave field by the Gaussian beam method is more or less influenced by several parameters which control the computations. The most important of them are the parameters which specify the properties of Gaussian beams used in the expansion, mainly the initial width of the Gaussian beam. The best way of appreciating the influence of these parameters on the final results is to perform test computations for simple structures by the Gaussian beam method, for which the properties of the wave field are well known. By varying the parameters, we can easily appreciate the sensitivity of the method to the parameters of computations.

Generally, we require that the parameters of computation do not influence the computed wave fields considerably. If this were not so, the method of Gaussian beams could not be used for

*) Address: Boční II, 141 31 Praha 4.

**) Address: Ke Karlovu 3, 121 16 Praha 2.

numerical modelling of seismic wave fields in laterally inhomogeneous media. However, we expect that some small influence will exist, and we must learn how to select the parameters of computation to obtain the results with the required accuracy.

The paper is divided into two parts. In this first part, referred to as Part I, we explain the method and present necessary mathematical background. We also describe shortly the computer program and certain pecularities of the numerical procedures. Finally, we describe the model used for computations and present and explain some test computation and comparison with exact results.

In the second part of the paper (referred to as Part II) which will be published later, a more detailed investigation of the sensitivity of the results to the parameters of computation will be given, see [5].

The model of the medium used in our test computation is very simple — a plane interface between two homogeneous halfspaces. We shall describe the results of the computation for reflected *PP*, *PS*, *SP* and *SS* waves. The main attention is, of course, paid to the reflected *PP* waves which play an important role in applications.

The three main questions which are investigated in Part I of the paper are as follows:

1) how the Gaussian beam method works in regions of regular behaviour of the ray field,

2) how the method works in the critical region which is a singular region in the ray method,

3) whether head waves are also obtained by a summation of the reflected Gaussian beams.

The numerical results presented in Sec. 4 (and in Part II) show that the method of Gaussian beams gives satisfactory results in all the three above — listed problems. In the regions of the regular ray field, the results of the Gaussian beam method practically coincide with the ray results. In the critical region, the Gaussian beam method gives the results predicted by exact methods. Let us mention, e.g., the frequency-dependent shift of the maximum of the amplitude-distance curve of reflected waves to larger distances, the smooth amplitude-distance curve just at the critical distance, etc. Finally, head waves are obtained by a superposition of reflected Gaussian beams. Notice that the head waves are not automatically included in the reflected wave field in the ray method [6], but must be evaluated independently. In the Gaussian beam approach, the reflected wave field includes automatically head waves due to the singularity of the reflection coefficient in the integrand of the expansion integrals.

As mentioned above, the sensitivity of the wave fields computed by the Gaussian beam method to the parameters of computation will be investigated in Part II. It will be shown there that the results are generally very stable with respect to those parameters. Only the initial width of the Gaussian beam has a certain smoothing influence on the wave field in the critical region and on the head waves. The position of the maximum of the amplitude-distance curve of the reflected waves is, however, quite stable, independent of the initial width of Gaussian beams. The wave field of head waves, as a rather inexpressive peculiarity of the reflected wave field, may be smoothed by an improper choice of the initial width of the Gaussian beams. This influence will be discussed in detail in Part II.

Note that some synthetic seismograms of the reflected *PP* waves for a similar model of the medium, evaluated by the superposition of the Gaussian packets, were presented in [7]. The quantitative investigation of the final wave field and of the sensitivity of the results to the parameters of computation was not presented there. Even though the head waves were not obtained in [7] (due to some smoothing of the reflecting wave field caused by the initial width of the Gaussian beams adopted being too small), the possibility to obtain the head waves for larger initial widths was predicted there. This prediction is fully substantiated by the results of this paper.

2. THEORETICAL CONSIDERATIONS

In this section, we shall describe the basic principles of the Gaussian beam method and summarize the equations used in our test computations. We shall first discuss shortly Gaussian beams in a smoothly laterally inhomogeneous media. We shall then modify these formulae to obtain equations for Gaussian beams reflected/transmitted at a plane interface between two homogeneous halfspaces. After this, we shall present the expansion for a wave field generated by a line source into Gaussian beams and specify all the equations for the model used in our test examples.

Although all the theory given in Sections 2.1 – 2.3 applies to the wave field generated by a line source in a 2-D medium, a modification is described in Sec. 2.3 which can be used to evaluate the wave field generated by a point source in a 2-D medium. All the examples presented in the paper apply to the case of a point source.

2.1. Elastodynamic Gaussian beams in a 2-D laterally inhomogeneous smooth medium

Let us introduce a general Cartesian coordinate system x, y, z with the unit vectors $\mathbf{e}_x$, $\mathbf{e}_y$, $\mathbf{e}_z$, respectively, and assume that the parameters of the medium do not depend on one coordinate, say y.

We shall select an arbitrary ray Ω corresponding to a P or S wave situated in the plane $y = 0$. Let the ray Ω be specified by some ray paramter φ, which may correspond, e.g., to a polar angle defining the initial direction of the ray Ω at some point O of the ray Ω. The angle φ is zero when the ray Ω is pointing downwards at O, and increases in the counter-clockwise direction. We introduce a ray-centered coordinate system s, n connected with the ray Ω in the following way (see Fig. 1): The coordinate s measures the arclength along the ray Ω from an arbitrary reference point (say O), n represents a length coordinate perpendicular to Ω at s. The basis

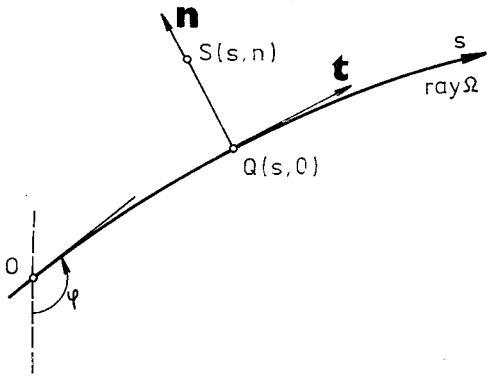

Fig. 1. The basis vectors $\mathbf{t}$, $\mathbf{n}$ of the ray-centered coordinate system s, n connected with the ray Ω specified by the ray parameter φ.

of the new 2-D coordinate system is formed by two unit vectors **t** and **n**, where **t** is a unit tangent and **n** the unit normal to the ray Ω. The vector **n** always points to the same side of the ray Ω so that rotation from **t** to **n** is counter-clockwise.

We denote by $\alpha(s)$, $\beta(s)$ and $\varrho(s)$ the velocities of P and S waves and the density, respectively, measured directly on the ray Ω. We also introduce a symbol $v(s)$ which has the meaning of $\alpha(s)$ when the ray Ω corresponds to a P wave, and $\beta(s)$ when it corresponds to an S wave.

Let us now consider an arbitrary point S situated in the plane $y = 0$ close to the ray Ω. The position of point S may be specified by the ray-centered coordinates (s, n). Point $Q(s, 0)$, situated on the ray Ω, will be referred to here as the projection of S on the ray Ω, see Fig. 1.

The displacement vector $\mathbf{u}(S, \varphi)$ at the point S, corresponding to the Gaussian beam concentrated close to the ray Ω (specified by the ray parameter φ) can be expressed as follows:

$$\mathbf{u}(S, \varphi) = u_1(S, \varphi)\, \mathbf{e}_1(Q, \varphi) + u_2(S, \varphi)\, \mathbf{e}_2(Q, \varphi)\,. \tag{1}$$

Here $u_1\mathbf{e}_1$ corresponds to the principal component of the displacement vector, $u_2\mathbf{e}_2$ to the additional component, see Fig. 2. For a P Gaussian beam, we have $\mathbf{e}_1 = \mathbf{t}$ and $\mathbf{e}_2 = \mathbf{n}$. For an SV Gaussian beam, $\mathbf{e}_1 = \mathbf{n}$ and $\mathbf{e}_2 = -\mathbf{t}$. Finally, for an SH beam, $\mathbf{e}_1 = \mathbf{e}_y$ and the additional component vanishes.

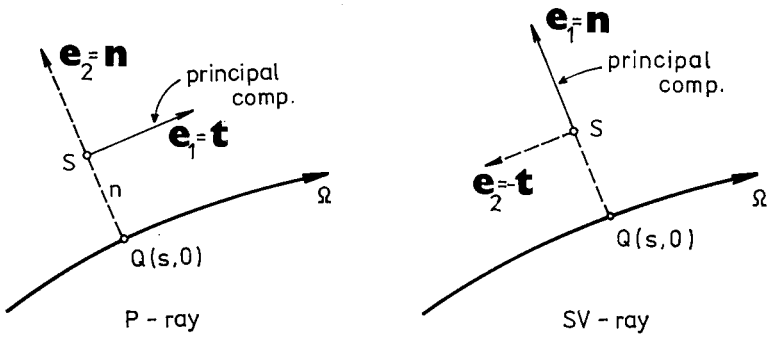

Fig. 2. The directions of the principal and additional components of the displacement vector for P- and SV-Gaussian beam, respectively.

For $u_1(S, \varphi)$ and $u_2(S, \varphi)$, we can write that

$$u_1(S, \varphi) = \Phi(\varphi)\,(v\varrho q)^{-1/2} \exp\left[\mathrm{i}\omega \int_0^s v^{-1}(\zeta)\,\mathrm{d}\zeta + \tfrac{1}{2}\,\mathrm{i}\omega n^2 p/q\right], \tag{2}$$

$$u_2(S, \varphi) = \Phi(\varphi)\, v^{1/2}(\varrho q)^{-1/2}\,(p/q)\, n \exp\left[\mathrm{i}\omega \int_0^s v^{-1}(\zeta)\,\mathrm{d}\zeta + \tfrac{1}{2}\,\mathrm{i}\omega n^2 p/q\right]. \tag{3}$$

The quantity $\Phi(\varphi)$ is a complex-valued constant, which remains constant along the whole ray Ω, but may vary from one ray to another. The integral in the exponential

function is taken along the ray Ω. For any given ray Ω, the quantities v, ϱ, p, q are functions of s only, not of n.

The quantities $p(s)$ and $q(s)$ are complex-valued solutions of the dynamic ray tracing system, see [8],

$$\mathrm{d}q/\mathrm{d}s = vp\,, \quad \mathrm{d}p/\mathrm{d}s = -v^{-2}v_{,nn}q\,, \tag{4}$$

where $v_{,nn}$ is the second derivative of the relevant velocity with respect to n.

It was shown in [3, 8] that complex-valued solution of the dynamic ray tracing system (4) in a homogeneous medium with the velocity v_0 can be expressed without a loss of generality as

$$q(s) = \varepsilon + s\,, \quad p(s) = 1/v_0\,, \tag{5}$$

where ε is some complex-valued constant with a negative imaginary part. It is convenient to express it as

$$\varepsilon = S_0 - \tfrac{1}{2}\,\mathrm{i}\omega_0 L_0^2/v_0\,, \tag{6}$$

where $\omega_0 = 2\pi(s^{-1})$ is the circular frequency corresponding to the frequency of 1 Hz. The quantities S_0 and L_0 are some real-valued constants.

Let us now explain the physical meaning of the quantities S_0 and L_0, as we shall use them frequently in this paper. The exponential term in Eqs. (2) and (3) can be rewritten as follows

$$\exp\left[\tfrac{1}{2}\,\mathrm{i}\omega n^2 p/q\right] = \exp\left[\tfrac{1}{2}\,\mathrm{i}\omega K n^2 - n^2 \mathrm{L}^{-2}\right], \tag{7}$$

where

$$K = \mathrm{Re}\,(p/q)\,, \quad L = \left[\tfrac{1}{2}\omega\,\mathrm{Im}\,(p/q)\right]^{-1/2}. \tag{8}$$

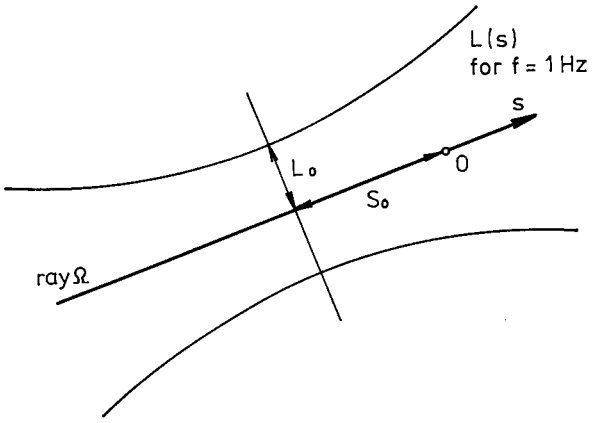

Fig. 3. Parameter $-S_0$ specifies the s-coordinate of the minimum width of the Gaussian beam, parameter L_0 is the halfwidth of the beam for the frequency 1 Hz at the point where the beam is the narrowest.

It is simple to see that $K(s)$ denotes the curvature of the wavefront of the Gaussian beam, and $L(s)$ is the effective halfwidth of the Gaussian beam. Both these quantities vary with s along the ray Ω, and they do not depend on n. In a homogeneous medium, we have, see (5) and (6),

$$L(s) = (2v_0/\omega)^{1/2} \left[\tfrac{1}{2} L_0^2 \omega_0 / v_0 + 2v_0 L_0^{-2} \omega_0^{-1} (S_0 + s)^2\right]^{1/2} . \tag{9}$$

As we can see from (9), the function $L = L(s)$ is a hyperbola, with a minimum at $s = -S_0$, see Fig. 3. Thus, in a homogeneous medium, $-S_0$ denotes the s-coordinate of the point where the Gaussian beam is narrowest. At point $s = -S_0$, we have, see (9),

$$[L(s)]_{s=-S_0} = L_0(\omega_0/\omega)^{1/2} . \tag{10}$$

Thus, the quantity L_0 has the meaning of the minimum effective half width of the Gaussian beam for a frequency of 1 Hz. The dimensions of S_0 and L_0 are lengths; we shall express them in kilometers.

2.2. Reflected-transmitted Gaussian beams

The above equations must be modified when we consider reflected-transmitted Gaussian beams. A detailed investigation of this problem can be found in [4], here we shall present only the final formulae, specified for our simple model of medium.

We shall consider a plane interface between two homogeneous halfspaces. We shall denote the incident Gaussian beam and the quantities related to this beam by the superscript I (I = incident). We select one of the reflected/transmitted beams and denote it and all the relevant quantities by the superscript R (R = reflected/transmitted). For the reflected-transmitted Gaussian beam we obtain the relations

$$\mathbf{u}^{\mathrm{R}}(S, \varphi) = u_1^{\mathrm{R}}(S, \varphi)\, \mathbf{e}_1 + u_2^{\mathrm{R}}(S, \varphi)\, \mathbf{e}_2 . \tag{11}$$

Again, $u_1^{\mathrm{R}}\mathbf{e}_1$ denotes the principal component, $u_2^{\mathrm{R}}\mathbf{e}_2$ the additional component. The meaning of the unit vectors $\mathbf{e}_1$, $\mathbf{e}_2$ is the same as in Eq. (1), however, these vectors are related to the central ray of the reflected/transmitted beam. For u_1^{R} and u_2^{R} we obtain

$$u_1^{\mathrm{R}}(S, \varphi) = \Phi(\varphi)\, R\left[v^{\mathrm{I}} \varrho^{\mathrm{I}} (\varepsilon + G)\right]^{-1/2} \exp\left[i\omega\tau^{\mathrm{R}} + \tfrac{1}{2} i\omega n^2 p^{\mathrm{R}}/q^{\mathrm{R}}\right] , \tag{12}$$

$$u_2^{\mathrm{R}}(S, \varphi) = v^{\mathrm{R}}(p^{\mathrm{R}}/q^{\mathrm{R}})\, n u_1^{\mathrm{R}}(S, \varphi) . \tag{13}$$

Here $\Phi(\varphi)$ is the same constant as in the expression for the incident Gaussian beam, R is the relevant reflection/transmission coefficient of plane waves, and the other quantities are given by the following equations, see also Fig. 4,

$$\tau^{\mathrm{R}} = l_0/v^{\mathrm{I}} + l_1/v^{\mathrm{R}} , \quad G = l_0 + (v^{\mathrm{R}}/v^{\mathrm{I}})(\cos\delta^{\mathrm{I}}/\cos\delta^{\mathrm{R}})^2\, l_1 , \tag{14}$$

$$p^{\mathrm{R}}/q^{\mathrm{R}} = \cos^2\delta^{\mathrm{I}} / \left[v^{\mathrm{I}}(\varepsilon + G)\cos^2\delta^{\mathrm{R}}\right] .$$

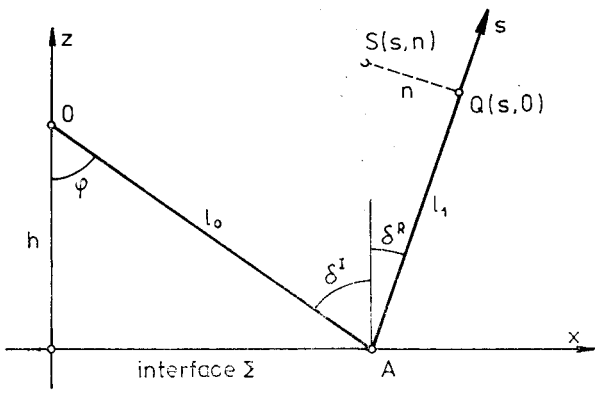

Fig. 4. The explanation of various symbols for incident and reflected Gaussian beams.

As shown in Fig. 4, δ^I and δ^R are the angles of incidence and of reflection/transmission, respectively. The relation between them is given by Snell's law,

$$\sin \delta^R = (v^R/v^I) \sin \delta^I . \tag{15}$$

The quantities l_0 and l_1 denote the lengths of the segments of the ray Ω between O and A and between A and Q, respectively.

2.3. Integral superposition of Gaussian beams

Before writing the expansion of the wave field generated by a line source into Gaussian beams, we shall introduce several notations. We shall specify the Cartesian coordinate system x, y, z introduced earlier in the following way. We put the interface into the coordinate plane $z = 0$ and assume that the z-axis is pointing upwards. The positive orientation of the x-axis is shown in Fig. 4 and the y-axis makes up the right-handed system x, y, z. We now assume that the line source, parallel with the y-axis, intersects the plane $y = 0$ at the point O at the z-axis, at a distance h from the interface Σ.

We assume now that the far-field approximation of the wave field generated by the line source at a distance r from the line source is given by the relation

$$\boldsymbol{U}(r) = r^{-1/2} \exp(i\omega r/v_0)\, \mathbf{e} , \tag{16}$$

where $\mathbf{e}$ is the unit vector specifying in an obvious way the direction of the displacement vector $\boldsymbol{U}$ for P, SV or SH waves.

The expansion of the wave field (16) generated by a line source into Gaussian beams may be obtained by a simple modification of the equations derived in [8]. It reads

$$\boldsymbol{U}(S) = (\tfrac{1}{2}\varepsilon\varrho_0\omega/\pi)^{1/2} \exp(\tfrac{1}{4}i\pi) \int_{\varphi_{MIN}}^{\varphi_{MAX}} \boldsymbol{u}(S, \varphi)\, d\varphi . \tag{17}$$

Here $\boldsymbol{u}(S, \varphi)$ is given by (1), (2) and (3), where we put $\Phi(\varphi) = 1$ and specify all the quantities for the homogeneous medium. Note one difference between expansion (17) and the expansion presented in [8]. Here we consider elastodynamic Gaussian beams with the amplitude factor $(v\varrho q)^{-1/2}$, whereas in [8] the wave equation and corresponding scalar Gaussian beams, with the amplitude factor $(v/q)^{1/2}$ were considered. This implies an additional factor $v_0\varrho_0^{1/2}$ in our equation (17). The detailed derivation and discussion of expansion (17) will be published elsewhere.

The integral in (17) is over the parameters of the ray φ, the integration limits φ_{MIN} and φ_{MAX} have been chosen in such a way that the Gaussian beams $\boldsymbol{u}(S, \varphi)$ with central rays outside these limits do not contribute effectively to the wavefield at S.

As the problem is linear, we can consider the propagation of Gaussian beams $\boldsymbol{u}(S, \varphi)$ in expansion (17) independently. The reflected/transmitted wave field is obtained analogously as a superposition of the reflected/transmitted Gaussian beams. In this way, for the displacement vector $\boldsymbol{U}^{\mathrm{R}}(S)$ of the reflected/transmitted wave at the point S, we obtain the following expression:

$$\boldsymbol{U}^{\mathrm{R}}(S) = (\tfrac{1}{2}\varepsilon\varrho_0\omega/\pi)^{1/2} \exp(\tfrac{1}{4}\mathrm{i}\pi) \int_{\varphi_{\mathrm{MIN}}}^{\varphi_{\mathrm{MAX}}} \boldsymbol{u}^{\mathrm{R}}(S, \varphi)\, \mathrm{d}\varphi\,, \tag{18}$$

where $\boldsymbol{u}^{\mathrm{R}}(S, \varphi)$ is a reflected/transmitted Gaussian beam given by relations (11)–(13), with $\Phi(\varphi) = 1$. Inserting (11)–(13) into (18) yields

$$\boldsymbol{U}^{\mathrm{R}}(S) = [\varepsilon\omega/(2\pi v_0)]^{1/2} \exp(\tfrac{1}{4}\mathrm{i}\pi) \int_{\varphi_{\mathrm{MIN}}}^{\varphi_{\mathrm{MAX}}} (\varepsilon + G)^{-1/2}\, R \times \tag{19}$$

$$\times\, (\mathbf{e}_1 + v^{\mathrm{R}} p^{\mathrm{R}} n \mathbf{e}_2/q^{\mathrm{R}}) \exp[\mathrm{i}\omega\tau^{\mathrm{R}} + \tfrac{1}{2}\mathrm{i}\omega n^2 p^{\mathrm{R}}/q^{\mathrm{R}}]\, \mathrm{d}\varphi\,.$$

The expressions τ^{R}, G, $p^{\mathrm{R}}/q^{\mathrm{R}}$ are given by (14), l_0, l_1 and n can be determined as follows

$$\begin{aligned} l_0 &= h/\cos\delta^{\mathrm{I}}\,, \\ l_1 &= [x(S) - h\tan\delta^{\mathrm{I}}] \sin\delta^{\mathrm{R}} \pm z(S)\cos\delta^{\mathrm{R}}\,, \\ n &= \mp[x(S) - h\tan\delta^{\mathrm{I}}] \cos\delta^{\mathrm{R}} + z(S)\sin\delta^{\mathrm{R}}\,. \end{aligned} \tag{20}$$

Here the upper sign corresponds to the reflected wave, the lower sign to the transmitted wave.

Equation (19) gives the final expression for the displacement vector of the reflected/ /transmitted wave in a 2-D medium if the wave field is generated by a line source. As is well known, the expression can be simply modified even for the case of a point source taking into account a transverse spreading, see [4]. We can rewrite (19) in the final general form applicable both to a line and a point source as follows:

$$\boldsymbol{U}^{\mathrm{R}}(S) = [\varepsilon\omega/(2\pi v_0)]^{1/2} \exp(\tfrac{1}{4}\mathrm{i}\pi) \int_{\varphi_{\mathrm{MIN}}}^{\varphi_{\mathrm{MAX}}} (\varepsilon + G)^{-1/2}\, RA_{\perp} \times \tag{21}$$

$$\times (\mathbf{e}_1 + v^{\mathrm{R}} p^{\mathrm{R}} n \mathbf{e}_2 / q^{\mathrm{R}}) \exp\left[i\omega\tau^{\mathrm{R}} + \tfrac{1}{2} i\omega n^2 p^{\mathrm{R}} / q^{\mathrm{R}}\right] \mathrm{d}\varphi ,$$

where

$$A_\perp = (l_0 + l_1 v^{\mathrm{R}} / v^{\mathrm{I}})^{-1/2} \quad \text{for a point source ,} \tag{22}$$

$$= 1 \quad \text{for a line source .}$$

From (21), it is easy to obtain the equations for the components of the displacement vector $\boldsymbol{U}^{\mathrm{R}}(S)$. Let us denote the x- and z-components of $\boldsymbol{U}^{\mathrm{R}}(S)$ for the P and SV waves by U_x^{R} and U_z^{R}, respectively. Similarly, we denote the y-component of $\boldsymbol{U}^{\mathrm{R}}(S)$ for the SH wave by U_y^{R}.

For P and SV waves, (21) yields

$$U_x^{\mathrm{R}}(S) = \left[\varepsilon\omega/(2\pi v_0)\right]^{1/2} \exp\left(\tfrac{1}{4} i\pi\right) \int_{\varphi_{\mathrm{MIN}}}^{\varphi_{\mathrm{MAX}}} (\varepsilon + G)^{-1/2} R A_\perp \times \tag{23}$$

$$\times (e_{1x} + v^{\mathrm{I}} p^{\mathrm{R}} n e_{2x} / q^{\mathrm{R}}) \exp\left[i\omega\tau^{\mathrm{R}} + \tfrac{1}{2} i\omega p^{\mathrm{R}} n^2 / q^{\mathrm{R}}\right] \mathrm{d}\varphi ,$$

$$U_z^{\mathrm{R}}(S) = \left[\varepsilon\omega/(2\pi v_0)\right]^{1/2} \exp\left(\tfrac{1}{4} i\pi\right) \int_{\varphi_{\mathrm{MIN}}}^{\varphi_{\mathrm{MAX}}} (\varepsilon + G)^{-1/2} R A_\perp \times \tag{24}$$

$$\times (e_{1z} + v^{\mathrm{I}} p^{\mathrm{R}} n e_{2z} / q^{\mathrm{R}}) \exp\left[i\omega\tau^{\mathrm{R}} + \tfrac{1}{2} i\omega n^2 p^{\mathrm{R}} / q^{\mathrm{R}}\right] \mathrm{d}\varphi ,$$

where e_{1x}, e_{1z} are the x- and z-components of the vector $\mathbf{e}_1$, e_{2x} and e_{2z} are the same components of the vector $\mathbf{e}_2$. For P-waves, they are given by relations

$$e_{1x} = \sin \delta^{\mathrm{R}} , \quad e_{1z} = \pm \cos \delta^{\mathrm{R}} , \tag{25}$$

$$e_{2x} = \mp \cos \delta^{\mathrm{R}} , \quad e_{2z} = \sin \delta^{\mathrm{R}} .$$

Similarly, for SV waves, we have

$$e_{1x} = \mp \cos \delta^{\mathrm{R}} , \quad e_{1z} = \sin \delta^{\mathrm{R}} , \tag{26}$$

$$e_{2x} = -\sin \delta^{\mathrm{R}} , \quad e_{2z} = \mp \cos \delta^{\mathrm{R}} .$$

The upper sign again corresponds to the reflected waves, the lower sign to the transmitted waves.

For the y-component of the SH wave we have

$$U_y^{\mathrm{R}}(S) = \left[\varepsilon\omega/(2\pi v_0)\right]^{1/2} \exp\left(\tfrac{1}{4} i\pi\right) \int_{\varphi_{\mathrm{MIN}}}^{\varphi_{\mathrm{MAX}}} (\varepsilon + G)^{-1/2} R A_\perp \times \tag{27}$$

$$\times \exp\left[i\omega\tau^{\mathrm{R}} + \tfrac{1}{2} i\omega n^2 p^{\mathrm{R}} / q^{\mathrm{R}}\right] \mathrm{d}\varphi .$$

3. NUMERICAL CONSIDERATIONS

Although a general program, BEAM81, to evaluate synthetic seismograms in 2-D laterally varying layered structures exists, see [7], it was found useful to write an independent, considerably simpler program called GB, to realize the procedures

outlined above. There are several reasons for this, we shall mention some of them. Firstly, several simplifications were used in BEAM81, which were based on the paraxial approximation. These approximations are not used in GB. Secondly, the tracing and dynamic ray tracing is performed numerically in BEAM81, whereas simple analytical solutions exist and are used in our model. This prevents some numerical inaccuracies from being generated. Thirdly, the presentation of results in the frequency domain shows more distinctly the differences between various results and the sensitivity of the results to various parameters of computations, which can be hardly recognized in synthetic seismograms.

In this section, we shall shortly describe several peculiarities of the program GB and explain some parameters we shall need in the description of numerical examples. The GB program was written by the first named author as part of her Diploma Thesis [9].

3.1. Discretization of the expansion expressions

The integrals (23) and (24) were evaluated by numerical quadratures. A regular increment $\Delta\varphi$ of the ray parameter φ was used. We shall write here only the discrete formula for the vertical component of the displacement vector $U_z^R(S)$. It reads

$$U_z^R(S) = [\varepsilon\omega/(2\pi v_0)]^{1/2} \exp(\tfrac{1}{4}i\pi)\, \Delta\varphi \sum_{k=0}^{N} \{(\varepsilon + G)^{-1/2} RA_\perp \times \times (e_{1z} + v^R p^R n e_{2z}/q^R) \exp[i\omega\tau^R + \tfrac{1}{2}i\omega n^2 p^R/q^R]\}_{\varphi=\varphi_k}, \tag{28}$$

where $\varphi_k = \varphi_0 + k\,\Delta\varphi$. The quantity $\Delta\varphi$ has been determined so that

$$\varphi_0 = \varphi_{\mathrm{MIN}}, \quad \varphi_N = \varphi_{\mathrm{MAX}}. \tag{29}$$

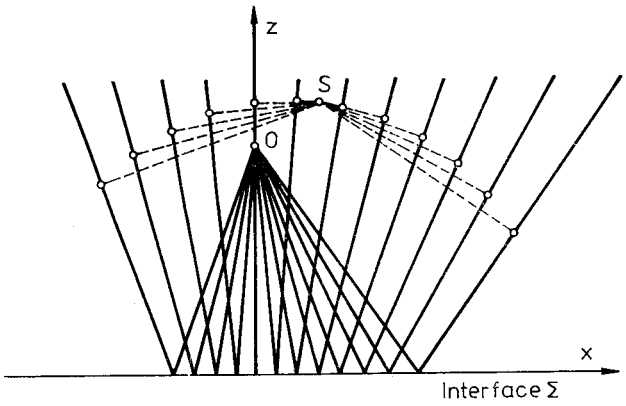

Fig. 5. The wavefield at point S is obtained as a superposition of Gaussian beams passing in the neighbourhood of S. The expansion includes both the beams leaving the source O to the left and to the right.

In this way, Eq. (28) represents a discrete expansion of the continuous wave field into Gaussian beams.

If the receiver S is situated close to the z-axis, i.e. if the epicentral distance x is small, the discrete expansion (28) includes both the beams which leave the source to the right ($\varphi > 0$) and to the left ($\varphi < 0$). For this reason, the angle φ_{MIN} was chosen negative in most of the numerical examples, see Fig. 5.

3.2. Windowing of Gaussian beams

Theoretically, Gaussian beams are infinitely broad. In the computation, however, it is possible to neglect those parts of Gaussian beams which are very far from the central ray, where their amplitudes are substantially smaller than on the central ray. In the GB program, a quantity a_0 was introduced which controls the windowing of Gaussian beams. The meaning of the quantity a_0 is as follows. The contribution of the Gaussian beam is neglected in those parts of the beam where the amplitude is smaller than $a_0 A_c$, A_c being the amplitude on the central ray. Figure 6 shows the "windowed" Gaussian beam for $a_0 = 0{\cdot}1$. The hatched part of the Gaussian beam is not used in the computations. We shall refer to the quantity a_0 as the parameter of the window.

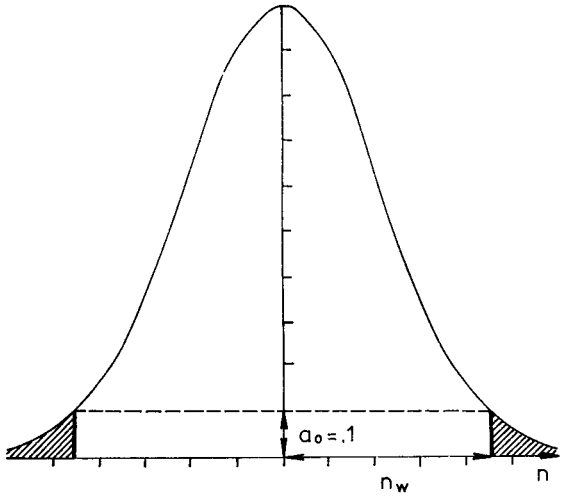

Fig. 6. The windowing of Gaussian beams for the parameter of the beam $a_0 = 0{\cdot}1$. The hatched part of the beam is not used in the computations.

As the Gaussian beam envelope is described by the relation $\exp(-n^2/L^2)$, see (7), we immediately see that the halfwidth of the window n_w is related to a_0 as follows:

$$n_w = L[\ln(1/a_0)]^{1/2}, \tag{30}$$

where L is the halfwidth of the Gaussian beam. Table 1 gives numerical examples of the relation between n_w and a_0. Note that the halfwidth of the window n_w equals the halfwidth of the beam L when $a_0 = 0{\cdot}37$.

Table 1. Values of the half-width of the window n_w for different parameters of the window a_0 for $L = 1$.

a_0	·01	·02	·03	·04	·05	·06	·07	·08	·09
n_w	2·15	1·98	1·87	1·79	1·73	1·68	1·63	1·59	1·55
a_0	·10	·20	·30	·40	·50	·60	·70	·80	·90
n_w	1·52	1·27	1·10	·96	·83	·71	·60	·47	·32

3.3. Elimination of distant Gaussian beams

Due to the windowing of Gaussian beams described in Sec. 3.2, it is not necessary to compute all the Gaussian beams in the expansion (28). When we evaluate the wave field at the point S, it is just possible to evaluate successively the coordinates n for all beams (for $\varphi_k = \varphi_0, \varphi_1, \ldots$) and take into account only those beams for which n is less than n_w, see (30). This will save computer time considerably. Only several beams passing in the neighbourhood of S need usually be considered to obtain reliable results.

3.4. Several comments on the numerical procedure

The amplitudes and phases of horizontal and/or vertical components of any reflected/transmitted wave at any point of the medium can be calculated simply using the numerical procedures described above. A point source or a line source may be considered. Both the principal and additional components are included in the computations. Optionally, the additional component need not be considered, and the wave field is expressed as the superposition of principal components only.

By a suitable selection of φ_{MIN} and φ_{MAX}, a reflected wave from a block structure may be approximately evaluated. In this case, the angle φ_{MIN} corresponds to the ray reflected from the left-hand edge of the block, and the φ_{MAX} to the ray reflected from the right-hand edge of the block. The results of computations of reflected waves from a block structure performed in this way by the GB program will be described elsewhere.

The procedure outlined above cannot be used for receivers situated close to the interface and/or for broad Gaussian beams, particularly if low frequencies are involved. In this case it may happen that the projection Q of point S on to the reflected ray would be situated on the opposite side of the interface, where the ray Ω does not exist physically. See example in Fig. 7. This limitation, however, can be removed by a modification which does not use the projections of point S on to the central rays

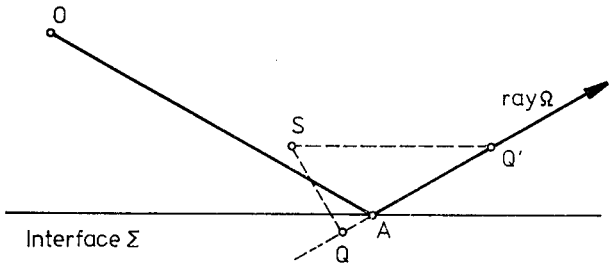

Fig. 7. The situation when the projection of S on the ray Ω does not exist. Formally, the reflected ray may be continued below the interface and point Q constructed on this fictitious ray. Another possibility is to modify the method of Gaussian beams and use for computations some other point on the ray Ω instead of the point Q (say, the point Q').

of the individual beams, but some other points on central rays. Such a modification is described in detail in [4]. It allows, e.g., the point Q' to use for evaluation, see Fig. 7. The only condition is that the point S is situated in the effective vicinity of Q'. By the effective vicinity of the point Q' we understand the circular region with its center at Q' and with a radius of $r = 0(\omega^{-1/2})$ for $\omega \to \infty$. All relevant formulae are given in [4].

Another possibility is to continue formally the reflected wave field along the fictitious ray to point Q situated below the interface. Then, point Q can be used in the Gaussian beam procedure without difficulties, although it is situated below the interface. This approach is included in the GB program as a standard option. Let us emphasize, however, that this situation occures in our computations very exceptionally, only for very broad Gaussian beams. More attention will be devoted to this problem in Part II.

4. NUMERICAL EXAMPLE

In this section, we shall present one numerical example of the computation of the *PP* reflected wave field. To appreciate the accuracy of the Gaussian beam procedure in the critical region, we shall compare the results with the results of computations performed by means of the exact method, see [6].

4. 1. Parameters of test computations

We shall consider the following parameters of the medium: $\alpha_1 = 6{\cdot}4$ km/s, $\alpha_2 = 8$ km/s, $\beta_i = \alpha_i/\sqrt{3}$, $\varrho_i = 1$ $(i = 1, 2)$. The point source and the receivers are situated at a distance of 30 km from the interface. Only the vertical component of the displacement vector of *PP* reflected wave is presented.

The other input data are chosen as follows: $\varphi_{MIN} = -34{\cdot}4$ degrees, $\varphi_{MAX} = 80{\cdot}2$ degrees, $\Delta\varphi = 0{\cdot}57$ degrees, $S_0 = 0$ km, $L_0 = 50(\alpha_1/\pi)^{1/2} = 71{\cdot}3$ km, $a_0 = 0{\cdot}1$. Only the principal component is considered, the additional component is not evaluated. The computations are performed for the frequency of $f = 6{\cdot}4$ Hz.

We do not present here computations for various selections of parameters. A detailed investigation of the sensitivity and stability of results with respect to various parameters will be presented in Part II, see [5]. Similarly, we deal only with the compressional *PP* reflected waves, other types of reflected wave fields (*PS*, *SP*, *SS*) will be investigated in Part II.

4. 2. Results of computations and their discussion

For a better orientation in the results of computations, we first present a simple scheme of several rays in our model of the medium, see Fig. 8.

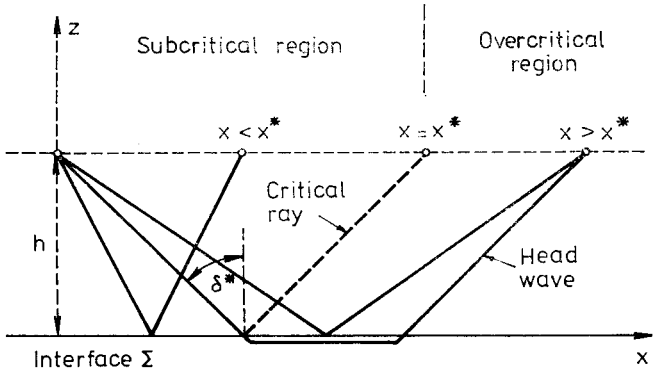

Fig. 8. Several rays in the model used for test computations. In the overcritical region, head waves are also generated.

A very important role is played by the critical ray, which corresponds to the critical angle of incidence $\delta^* = \arcsin(\alpha_1/\alpha_2)$. In our case, the critical ray intersects the profile of the receivers at the epicentral distance of $x^* = 80$ km (so-called critical distance). The characteristic peculiarities of the wave field are rather different at subcritical epicentral distances ($x < x^*$) and at overcritical epicentral distances ($x > x^*$). At subcritical distances, we have only the reflected waves, but at overcritical distances, a head wave is also generated. It is well-known that the ray theory fails in the vicinity of the critical ray (critical region), as the ray field is singular there. The reflected and head waves have quite different properties. In the terminology of the ray theory, the reflected waves are zero-order waves, but the head waves are a first-order approximation. In other words, this means that the reflected waves have the same normalized amplitude spectrum as the incident wave, but the amplitude spectrum of head waves has an additional factor $(1/i\omega)$. In the limit $\omega \to \infty$, the head waves vanish. In the ray methods, both the reflected waves and the head waves are investigated independently, as two different waves.

The ray amplitude-distance curves of waves under consideration for the above described model are presented in Fig. 9a for the frequency of 6·4 Hz. For comparison, also the exact amplitude-distance curve is shown. The figure is taken from [6].

The standard zero-order ray amplitude-distance curve of the *PP* reflected wave is shown by the bold dashed line. A most prominent feature of this curve is a distinct sharp maximum at the critical distance $x = 80$ km.

In the overcritical region $x > x^*$, the ray theory also predicts the head wave. The head wave reaches an infinite amplitude at the critical distance (where the ray method is singular) and then decreases continously. The ray amplitude-distance curve of the head wave is shown in Fig. 9a

by the thin dashed line, starting from some distance beyond the critical point. For the time-harmonic wave field we are considering here, the head waves interfere with the reflected waves. The resulting interference reflected-head wave has a typical oscillatory form. The oscillations are frequency dependent. The amplitude-distance curve of the interference reflected-head wave, evaluated by the ray method (by the first order approximation!) is shown in Fig. 9a by the thin dashed line.

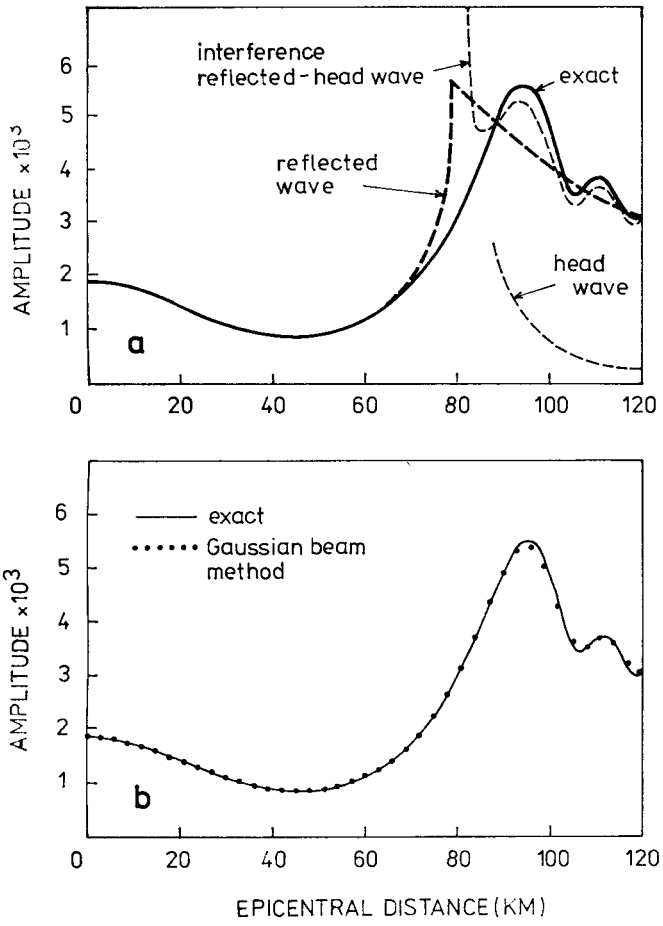

Fig. 9. Top figure (9a): Amplitude-distance curve of *PP*-reflected wave in the model under consideration computed by exact methods (bold continuous line) in comparison with some ray computations. The frequency is $f = 6{\cdot}4$ Hz, other parameters of computations are specified in the text. Bold dashed line shows the amplitude-distance curve of the reflected *PP* wave computed by the ray method (zero-order approximation). At the overcritical distance, the thin dashed lines denote the amplitude-distance curves of the head wave and of the interference reflected-head wave, computed by the ray method (first order approximation). The figure is taken from [6].

Bottom figure (9b): Amplitude-distance curve of *PP*-reflected wave in the model under consideration computed by the exact method (bold continous line) and by the method of Gaussian beams (dots). Both methods give practically identical results. The frequency is $f = 6{\cdot}4$ Hz.

The ray method does not give accurate results in the critical region, where the ray field is singular. The bold continuous line in Fig. 9a shows the amplitude curve of the *PP* reflected wave computed by exact methods. The method is based on numerical integrations in the complex plane along specially deformed integration contours, see [6] for larger details. The amplitude-distance curve of the reflected wave computed by the exact method is quite smooth and continuous in the neighbourhood of the critical point and reaches its maximum value at a certain distance beyond the critical point. The position of the maximum of the amplitude-distance curve is frequency-dependent. The greater the frequency, the closer the maximum is to the critical point.

In Fig. 9b, the exact amplitude-distance curve (shown again by the bold continuous line) is compared with the results of computations by the method of Gaussian beams. The results obtained by the method of Gaussian beams are shown by dots in Fig. 9b. As we can see, the Gaussian beam method gives practically the same results as the exact method.

5. CONCLUSIONS

Now, using Figs. 9a, b, let us draw some conclusions regarding our computations of the *PP*-reflected wave field by the Gaussian beam method.

In the region of regular behaviour of the ray field (subcritical epicentral distances) the Gaussian beam method is in excellent agreement with the ray method. The results of both methods coincide with an accuracy to several digits. As the results of the ray method are sufficiently accurate in this region (see Fig. 9a), the conclusion is that the Gaussian beam method can be safely used in the region of the regular ray field.

In the critical region, the results of the Gaussian beam method coincide with sufficient accuracy with the exact computations, see Fig. 9b. The conclusion is that the Gaussian beam method predicts correctly the reflected wave field even in the singular critical region. This is the most important conclusion of this paper. It should be emphasized that the wave field in the critical region is computed in the Gaussian beam method by the same algorithms as outside the critical region, and that it is not necessary to specify whether the receiver is situated in the critical region or not. Moreover, the Gaussian beam approach, used here only for a very simple model, can be generally used for arbitrary, laterally inhomogeneous models with curved interfaces, and for other types of reflected waves (*PS*, *SP*, *SS*).

At overcritical distances, the amplitude-distance curve of the interference reflected-head wave oscillates due to the existence of head waves, see Fig. 9a. As we can see, the oscillations also appear in the results obtained by the Gaussian beam method. Thus, the head waves are automatically included in the superposition of the reflected Gaussian beams, in contrast to the ray methods, where the head waves must be computed independently. This is the great advantage of the Gaussian beam method.

As is known, pure head waves are generated only at a strictly plane interface between two strictly homogeneous halfspaces. Under actual conditions, however, such a situation is rather rare; the interface is usually slightly curved and the velocities change slightly with the coordinates. The amplitudes of head waves are very sensitive to these slight changes. The waves obtained in seismic measurements which have travel-time curves very similar to those of pure head waves do not, as a rule, cor-

respond to pure head waves, but to some other types of waves, with rather different amplitude properties. Thus, the problem whether pure head waves are obtained in our simple model is more of academic interest than of practical importance. It is, however, a pleasure to see that the Gaussian beam method yields this interesting phenomenon.

It will be shown in Paper II that the pure head waves, as a inexpressive peculiarity of the reflected wave field, are more sensitive to the choice of parameters of computations than the reflected wave field itself. Some change of the parameters of computations can smooth the results. This smoothing practically does not change the general form of the amplitude-distance curve of the reflected waves and gives sufficiently accurate results even in the critical region, but may remove to some extent or fully the oscillations of the amplitude-distance curves at overcritical distances. In other words, it usually leads to some decrease of the amplitudes of head waves. This is the main reason why the head waves were not obtained in the computations presented in [7]. More detailed investigation of this effect will be performed in Part II of this paper, see [5].

Received 13. 5. 1983 *Reviewer: I. Pšenčík*

References

[1] N. J. Kirpichnikova: Construction of Solutions Concentrated Close to Rays for the Equations of Elasticity Theory in an Inhomogeneous Isotropic Space. Matem. voprosy teorii difrakcii i rasprostranenija voln, T. 1, Nauka, Leningrad 1971 (English Translation by Am. Math. Soc. 1974).

[2] V. Červený: Seismic Wave Fields in Structurally Complicated Media. (Ray and Gaussian Beam Approaches.) Lecture Notes, Vening-Meinesz Laboratory, Utrecht 1981.

[3] V. Červený, I. Pšenčík: Gaussian Beams in Two-Dimensional Elastic Inhomogeneous Media. Geoph. J.R. Astr. Soc., 72 (1983), 417.

[4] V. Červený, I. Pšenčík: Gaussian Beams in Two-Dimensional Laterally Varying Layered Structures. Geoph. J.R. Astr. Soc., (in print).

[5] J. Konopásková, V. Červený: Numerical Modelling of Time-Harmonic Seismic Wave Fields in Simple Structures by the Gaussian Beam Method, Part II. Studia geoph. et geod., 28 (1984), (in print).

[6] V. Červený, R. Ravindra: Theory of Seismic Head Waves. Univ. Toronto Press, Toronto 1971.

[7] V. Červený: Synthetic Body Wave Seismograms for Laterally Varying Layered Structures by the Gaussian Beam Method. Geoph. J.R. Astr. Soc., 73 (1983), 389.

[8] V. Červený, M. M. Popov, I. Pšenčík: Computation of Wave Fields in Inhomogeneous Media — Gaussian Beam Approach. Geoph. J.R. Astr. Soc., 70 (1982), 109.

[9] J. Hronová: Výpočet vlnových polí v jednoduchých strukturách metodou gaussovských svazků. Diplomová práce, Mat. fyz. fakulta Univ. Karlovy, Praha 1982 (not published).